Dennis, P. Shah, US 5773239A, June 30, **1998** [*Chem. Abstr.* **1998**, 129, 95683].
[2] S. M. Colegate, P. R. Dorling, C. R. Huxtable, *Austr. J. Chem.* **1979**, *32*, 2257.
[3] A. D. Elbein, R. D. Molyneux in *Iminosugars as Glycosidase Inhibitors; Nojirimycin and Beyond* (Eds.: A. E. Stütz), Wiley-VCH, Weinheim, **1999**, Chap. 11, p. 216.
[4] See, for example: P. E. Goss, J. Baptiste, B. Fernandes, M. Baker, J. W. Dennis, *Cancer Res.* **1994**, *54*, 1450; P. E. Goss, C. L. Reid, D. Bailey, J. W. Dennis, *Clin. Cancer Res.* **1997**, *3*, 1077; P. D. Rye, N. V. Bovin, E. V. Vlasova, R. A. Walker, *Glycobiology* **1995**, *5*, 385; J. W. Dennis, M. Granovsky, C. E. Warren, *BioEssays* **1999**, *21*, 412; J. W. Dennis, M. Granovsky, C. E. Warren, *Biochim. Biophys. Acta* **1999**, *1473*, 21.
[5] W. H. Pearson, L. Guo, *Tetrahedron Lett.* **2001**, *42*, 8267; W. H. Pearson, E. J. Hembre, *Tetrahedron Lett.* **2001**, *42*, 8273.
[6] C. W. Ekhart, M. H. Fechter, P. Hadwiger, E. Mlaker, A. E. Stütz, A. Tauss, T. M. Wrodnigg in *Iminosugars as Glycosidase Inhibitors; Nojirimycin and Beyond* (Eds.: A. E. Stütz), Wiley-VCH, Weinheim, **1999**, Chap. 12, p. 253.
[7] F. Popowycz, S. Gerber-Lemaire, R. Demange, E. Rodriguez-Garcia, A. T. Carmona Asenjo, I. Robina, P. Vogel, *Bioorg. Med. Chem. Lett.* **2001**, *11*, 2489.
[8] For a related study, see: C. Saotome, C. H. Wong, O. Kame, *Chem. Biol.* **2001**, *138*, 1; see also: G. Limberg, I. Lindt, J. Zavilla, *Synthesis* **1999**, 178.
[9] J. Hine, F. A. Via, *J. Am. Chem. Soc.* **1972**, *94*, 190; J. Hine, C. Y. Yeh, F. C. Schmalstieg, *J. Org. Chem.* **1970**, *35*, 340; J. Hine, C. Y. Yeh, *J. Am. Chem. Soc.* **1967**, *89*, 2669; E. Gout, M. Zador, C. G. Beguin, *Nouv. J. Chim.* **1984**, *8*, 243.
[10] A. Ganessan, *Angew. Chem.* **1998**, *110*, 2989; *Angew. Chem. Int. Ed.* **1998**, *37*, 2828; J. M. Lehn, *Chem. Eur. J.* **1999**, *5*, 2455; V. A. Polyakov, M. I. Nelen, N. Nazarpack-Kandlousy, A. D. Ryabov, A. V. Eliseev, *J. Phys. Org. Chem.* **1999**, *12*, 357; A. V. Eliseev, J. M. Lehn, *Curr. Top. Microbiol. Immunol.* **1999**, *213*, 159; C. Karan, B. L. Miller, *Drug Discovery Today* **2000**, *5*, 67; J. M. Lehn, *Science* **2001**, *291*, 2331, and references cited therein; P. A. Brady, R. P. Bonar-Law, S. J. Rowan, C. J. Suckling, J. K. Sanders, *Chem. Commun.* **1996**, 319; S. J. Rowan, P. A. Brady, J. K. M. Sanders, *Angew. Chem.* **1996**, *108*, 2283; *Angew. Chem. Int. Ed. Engl.* **1996**, *35*, 2143.
[11] For related studies showing similar autocatalytical effects, see: J. Hine, M. S. Cholob, W. K. Chess, Jr., *J. Am. Chem. Soc.* **1973**, *95*, 4270.
[12] This commercially available enzyme is a useful model for α-mammalian α-mannosidases such as Golgi α-mannosidase II; see, for example: S. Howard, S. He, S. G. Withers, *J. Biol. Chem.* **1998**, *273*, 2067.
[13] For details of the enzymatic assays, see: A. Brandi, S. Cicchi, F. M. Cordero, B. Frignoli, A. Goti, S. Picasso, P. Vogel, *J. Org. Chem.* **1995**, *60*, 6806; S. Picasso, Y. Chen, P. Vogel, *Carbohydrate Lett.* **1994**, *1*, 1; see also : J. E. Tropea, R. J. Molyneux, G. P. Kaushal, Y. T. Pan, M. Mitchell, A. D. Elbein, *Biochemistry* **1989**, *28*, 2027.
[14] The same assays were made on *N*-methylpyrrol-2-carbaldehyde and *N*-(*tert*-butyloxycarbonyl)pyrrolidine-2-carboxaldehyde. No significant inhibitory activities were observed.
[15] G. W. J. Fleet, J. C. Son, D. St. C. Green, I. Cenci di Bello, B. Winchester, *Tetrahedron* **1988**, *44*, 2649.

Received: December 10, 2001 [Z330]

A Three-State Mechanism of Integrin Activation and Signal Transduction for Integrin $\alpha_v\beta_3$

Kay E. Gottschalk, Robert Günther, and Horst Kessler*[a]

KEYWORDS:

docking · drug research · integrins · signal transduction · molecular modeling

Integrins are membrane-spanning heterodimeric receptors which couple signal transduction with cell matrix adhesion. Several integrins recognize the tripeptide sequence in RGD-containing peptides and proteins. However, the atomic detail of the ligand binding site is currently unknown. Starting from the crystal structure of the extracellular domains of the integrin $\alpha_v\beta_3$, we develop a three-state mechanism of integrin activation based on Ca^{2+} displacement upon ligand binding. We present a detailed working model of the highly important but poorly understood mechanism of an integrin signaling event. Additionally, we describe the ligand binding site in atomic detail, which might be a first step in future rational drug design attempts.

In a recent pioneering work, Xiong et al. solved the crystal structure of the extracellular domains of $\alpha_v\beta_3$ (Protein Data Bank (pdb) entry 1JV2),[1] which provides the possibility of looking at integrin-activating processes at the atomic level (Figure 1 A). Currently, the consensus model for integrin activation and signal transduction is a two-state mechanism: a low-affinity resting state (state one) is activated by intracellular events that lead to a high-affinity binding state (state two) after a conformational change. This activation process involves the separation of the α_v propeller domain and the β_3 βA domain[2–4] (the so-called head groups, Figure 1 B). However, biochemical investigations also support a model with multiple activation states.[5, 6] Here, we start from the crystal structure of the extracellular domains of $\alpha_v\beta_3$ and use automated docking and molecular modeling to develop a three-state mechanism involving allosteric effects triggered by a ligand-induced shift of a Ca^{2+} ion. We introduce an additional step before dissociation of the head groups, which corresponds to the crystal structure and constitutes a high-affinity state.

In our model, the inactive state (state one, Figure 1 C, left) is locked in its position by intracellular interactions.[7] Proteins binding at intracellular domains[4, 8] trigger a rotational movement of an integrin subunit, which activates the integrin. This activated or preconditioned state (state two, Figure 1 C, middle)

[a] *Dr. H. Kessler, Dipl. Chem. K.-E. Gottschalk[+], Dr. R. Günther[+]*
Institut für Organische Chemie und Biochemie
TU München
Lichtenbergstrasse 4
85747 Garching (Germany)
Fax: (+49) 89-289-13210

[+] *These authors contributed equally to this work.*

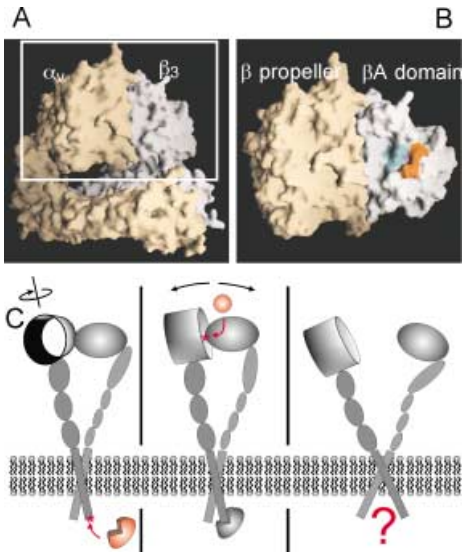

Figure 1. ***A****) Crystal structure of the extracellular domains of integrin $\alpha_v\beta_3$. The α subunit is shown in yellow, the β subunit in white, and the Ca^{2+} ion bound to the adMIDAS region in magenta.* ***B****) Docking studies were performed on the head groups of integrin $\alpha_v\beta_3$, which comprise the β propeller domain of α_v and the βA domain of β_3. The MIDAS region is depicted in blue, the adMIDAS region in orange.* ***C****) Three-state model of signal transduction in integrins. In accordance with experimental and theoretical studies, intracellular proteins attach to $\alpha_v\beta_3$ and trigger a rotational movement of the head groups, which exposes the extracellular ligand binding site (left). Binding of ligands at this site (middle) leads to conformational changes in the head group region, which in turn evokes separation of the integrin subunits (right). This separation might be a starting point for further intracellular events.*

corresponds to the published crystal structure and has a high affinity for extracellular ligands. In contrast to the prevailing model, the head groups are still associated in this state. Extracellular ligand binding leads to further conformational changes, which separate the integrin head groups (state three, Figure 1 C, right).[9a] This is in complete accord with recent molecular modeling studies of the transmembrane domains, which show that these domains can adopt three states. Two of these transmembrane conformations, which correspond in our model to the inactive and activated state, respectively, differ only in the relative rotation of the transmembrane helices, while the conformation of the third state, which has separated head groups, also has a higher crossing angle between the helices.[9b]

It has been postulated that a Ca^{2+} ion bound to the metal-ion-dependent adhesion site (MIDAS) region of the βA domain of the integrin subunit β_3 interacts with the aspartic acid of RGD peptides and with the receptor.[10] Surprisingly, the MIDAS region of βA, in contrast to a region nearby called the adMIDAS region, is not populated by a metal ion in the crystal structure of $\alpha_v\beta_3$.[1] Further studies showed that the N-terminal β propellers of the α subunits are also involved in the process of binding ligands and that the arginine of the tripeptide sequence RGD binds in this region.[11–13] While the distance between the arginine and aspartic acid in cyclic RGD peptides is about 13 Å,[14–16] the shortest distance between the Ca^{2+} ion bound to the adMIDAS region and the β propeller of subunit of α_v is in the order of 17 Å. Thus, it seems that the crystal structure does not constitute the final ligand binding conformation of the receptor.

Superposition of the βA domain of the β_3 subunit and of the I domain of integrin α_2 reveals a high structural similarity between these two structures (Figure 2 a).[17] Analysis of the structures of the free I domain of α_2 integrin and the same I domain in complex with collagen shows that the binding of the ligand results in movement of the Ca^{2+} ion and the MIDAS region of the I domain. We propose that a similar conformational change occurs in the case of the β_3 subunit, which should lead to a displacement of the Ca^{2+} ion. To corroborate this hypothesis we modeled the β_3 MIDAS region according to the I domain of α_2

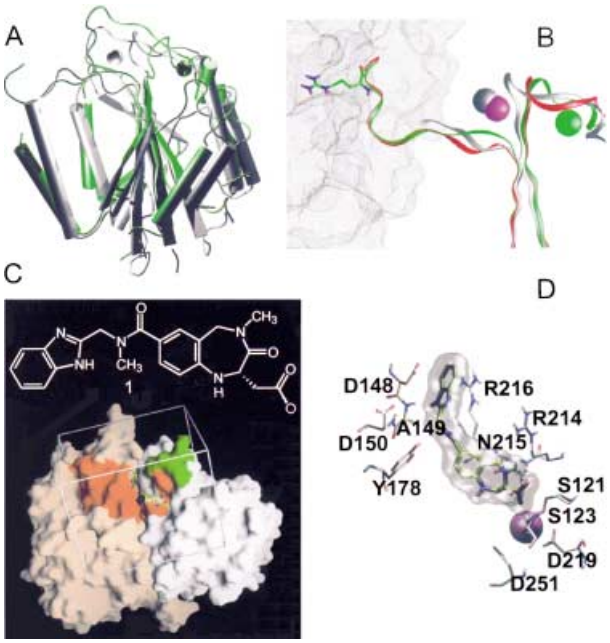

Figure 2. ***A****) Superposition of the I domain of collagen-associated integrin subunit α_2 (grey) with the βA domain of integrin subunit β_3 (green). The respective metal ions are depicted as spheres; the grey sphere represents the metal ion bound to the MIDAS region of α_2, the green sphere the ion bound to the adMIDAS region of β_3. The backbone root-mean-square deviation of the superimposed residues is 1.6 Å despite the large difference in metal position.* ***B****) Superposition of the metal-coordinating regions of integrin α_2 (grey), the crystal structure of the β_3 domain (green), and the structure of the β_3 domain that was modeled with regard to integrin α_2 (red). The original Ca^{2+}-ion position is indicated by a green sphere; the position of the shifted Ca^{2+} ion is shown as a red sphere and is nearly identical to the respective metal position in integrin α_2 (shown in grey). The surface of the α_v subunit and the position of the (β)-Arg^{261} residue are also shown. The Ca^{2+} ion is moved towards the α_v subunit, which allows ligand interactions with both integrin subunits. The proximity of the shifted loops to the (β)-Arg^{261} residue implies an allosteric effect of ligand binding on this arginine, which in turn may trigger dissociation of the integrin head groups.* ***C****) Binding of* ***1*** *to the head groups of the integrin $\alpha_v\beta_3$ obtained by automated docking carried out by employing the AutoDock 3.0 program.[29] Regions which are expected to be involved in ligand binding (residues 142 – 151 and 172 – 181 in integrin α_v and 179 – 181 and 214 – 217 in the β_3 subunit) are shown in red. The so-called 'specificity region' of the β_3 subunit is green. Initial docking simulations on the whole heterodimer confirmed that the binding site is close to the MIDAS region of the β_3 subunit (data not shown).* ***D****) Most favorable binding arrangement of ligand* ***1*** *to integrin $\alpha_v\beta_3$ as determined by automated docking. Interacting residues of the α_v domain are depicted in orange, residues of the β_3 domain in grey. The Ca^{2+} ion in the shifted MIDAS region is shown in magenta. The acidic moiety of* ***1*** *now takes part in Ca^{2+} coordination at the MIDAS region. The other interacting residues have been shown to be involved in ligand binding by experimental studies.*

(Figure 2b) and performed automated docking studies of the $\alpha_v\beta_3$-selective inhibitor **1**[18] on this conformation associated with the α_v propeller domain (Figure 2c). Indeed, the acidic moiety of the ligand binds to the Ca^{2+} ion positioned in the shifted MIDAS region, while the portion corresponding to the arginine in the natural ligand binds in the region of the (α)-Asp^{148} and (α)-Tyr^{178} residues of the α_v propeller domain (Figure 2d). These regions have been shown to be crucial for ligand binding and subunit specificity.[19–21] A closer investigation of the modeled receptor conformation reveals that the adMIDAS region is no longer capable of Ca^{2+} binding, as the formerly calcium-complexing residue (β)-Asp^{127} is now pointing in the opposite direction compared to its position prior to ligand binding. Furthermore, the affinity of the MIDAS region for metal ions should increase as the (β)-Asp^{251} residue now takes part in metal complexation. The proposed Ca^{2+} displacement explains the influence of ion concentration on ligand binding. Low calcium concentrations support binding, whereas high calcium concentrations result in inhibition of ligand binding.[22, 23] Above a critical ion concentration the low-affinity MIDAS region close to the adMIDAS region will be populated in addition to the adMIDAS region prior to the ligand binding event, which will render the conformational changes impossible.

It has been shown that the specificity of cyclic RGD peptides correlates with the angle between the Lys and Asp residue.[24] As our model can only approximate the energies of binding due to inaccuracies in side chain conformations and negligence of solvent effects, we can only qualitatively show specificity effects. Comparing the conformations with our binding model rationalizes the following findings.: the $\alpha_v\beta_3$-specific RGD peptide adopts a conformation that is comparable to the synthetic ligand while the extended conformation of the $\alpha_{IIb}\beta_3$-specific RGD peptide cannot bind to $\alpha_v\beta_3$ in a similar fashion (Figure 3). Nevertheless, a structure with associated head groups is not in accordance with electron microscopy images of 'activated' integrins.[9, 25] Therefore, it seems likely that the ligand binding event leads to still further conformational changes of the integrin. Two loops that are involved in Ca^{2+} complexation are close to the (β)-Arg^{261} residue, which is part of the α/β interface and inserts into the β propeller of the α_v subunit. The (β)-Arg^{261} residue is surrounded by aromatic residues from this β propeller domain. Thus, cation–π interactions[26] between (β)-Arg^{261} and neighboring residues from the α_V subunit should contribute to the α/β interface.[1] A slight change in the position of the (β)-Arg^{261} residue induced by allosteric rearrangement caused by ligand binding and calcium displacement can disrupt these cation–π interactions. Consequently, the head groups dissociate, which leads to an increase of the crossing angle between the integrin subunits as observed in experimental and theoretical investigations. It has been shown in molecular modeling studies that involve the transmembrane regions of the homologous $\alpha_{IIb}\beta_3$ integrin that high activation energy is necessary for the transition from a small to a large crossing angle of the transmembrane helices (unpublished results). This energy may be provided by the ligand binding event.

In conclusion, we have developed a model of an integrin activation mechanism in structural terms based on the observation that conformational changes of the activated integrin are a necessity for ligand binding. Our mechanism is completely consistent with experimental data currently in the literature. The conformational changes involve a shift in the position of a metal ion from the recently described adMIDAS region to the MIDAS region of the β_3 subunit. A Ca^{2+} ion moves towards the α subunit, allowing ligand interactions with both subunits. The ion shift is accompanied by rearrangements of loops surrounding the MIDAS region, which in turn may trigger the dissociation of the integrin head groups. Thus, we show that the crystal structure is only a snapshot in a multistage process. Here, we used molecular modeling to fill in the steps between the x-ray structure and the ligand binding and activation mechanism.

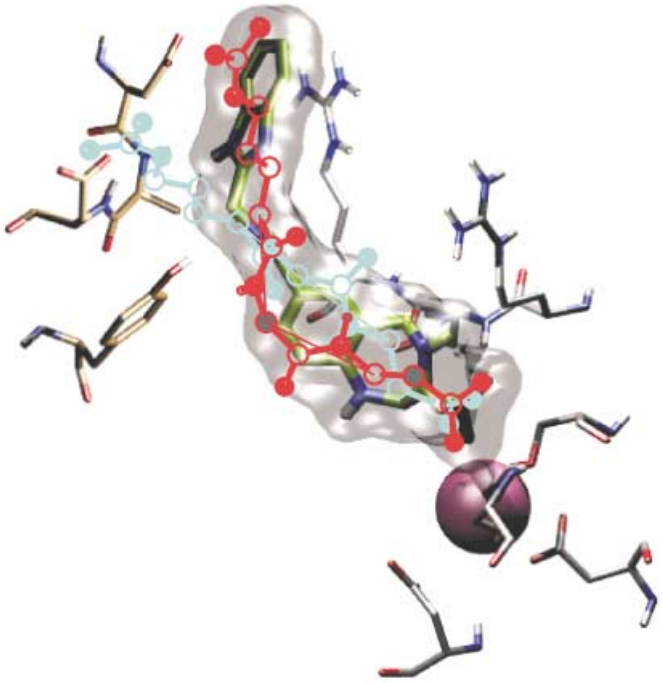

Figure 3. ***A****) Manual superposition of* ***1*** *and the RGD conformation of $\alpha_v\beta_3$-specific (red) and $\alpha_{IIb}\beta_3$-specific (cyan) cyclic RGD peptides. While the $\alpha_v\beta_3$-specific ligand adopts a conformation similar to the nonpeptidic ligand, the $\alpha_{IIb}\beta_3$-specific ligand cannot occupy the binding pocket.*

Methods

The β_3 backbone was threaded onto the α_2 conformation by employing the molecular modeling software tool MODELLER.[27] Sidechains of the affected residues were initially positioned by using the CONFMAT program[28] with 20 cycles. Conversion of these positions to the meanfield energy was achieved. Afterwards, 250 steps of conjugate gradient minimization were employed with harmonically restrained backbone atoms. Residues that were not affected by the loop modifications were kept fixed during minimization. The modeling software Sybyl 6.6 (Tripos Inc., St. Louis) was used to add polar hydrogens, to assign template charges, and to perform a geometry relaxation of the protein. The ligand was modeled in the same way.

To identify the ligand binding site in greater detail an automated docking of the inhibitor **1** was performed in a grid box of 38 × 40 ×

  1439-4227/02/03/05 $ 20.00+.50/0 ChemBioChem **2002**, No. 5

40 Å centred around the MIDAS region with a grid point spacing of 0.375 Å. The ligand was subjected to 50 docking runs by employing a Lamarckian Genetic Algorithm with all relevant torsional angles released and the various ring conformations of the inhibitor taken into account. Each docking run was initiated with a population of 50 individuals chosen at random and iterated through 7.5×10^6 energy evaluations. Up to 300 iterations of local search were applied with a frequency of 0.07. Thus, approximately 2×10^9 ligand – protein arrangements were evaluated.

[1] J. P. Xiong, T. Stehle, B. Diefenbach, R. Zhang, R. Dunker, D. L. Scott, A. Joachimiak, S. L. Goodman, M. A. Arnaout, *Science* **2001**, *294*, 339.
[2] R. C. Liddington, L. A. Bankston, *Exp. Cell Res.* **2000**, *261*, 37.
[3] E. F. Plow, T. A. Haas, L. Zhang, J. Loftus, J. W. Smith, *J. Biol. Chem.* **2000**, *275*, 21 785.
[4] S. J. Shattil, H. Kashiwagi, N. Pampori, *Blood* **1998**, *91*, 2645.
[5] D. Boettiger, F. Huber, L. Lynch, S. Blystone, *Mol. Biol. Cell* **2001**, *12*, 1227.
[6] D. Boettiger, L. Lynch, S. Blystone, F. Huber, *J. Biol. Chem.* **2001**, *276*, 31 684.
[7] P. E. Hughes, F. Diaz-Gonzalez, L. Leong, C. Wu, J. A. McDonald, S. J. Shattil, M. H. Ginsberg, *J. Biol. Chem.* **1996**, *271*, 6571.
[8] M. J. Humphries, *Biochem. Soc. Trans.* **2000**, *28*, 311.
[9] a) J. W. Weisel, C. Nagaswami, G. Vilaire, J. S. Bennett, *J. Biol. Chem.* **1992**, *267*, 16 637; b) K.-E. Gottschalk, P. D. Adams, A. T. Brunger, H. Kessler, *Protein Sci.* **2002**, in press.
[10] E. C. Tozer, R. C. Liddington, M. J. Sutcliffe, A. H. Smeeton, J. C. Loftus, *J. Biol. Chem.* **1996**, *271*, 21 978.
[11] J. C. Loftus, C. E. Halloran, M. H. Ginsberg, L. P. Feigen, J. A. Zablocki, J. W. Smith, *J. Biol. Chem.* **1996**, *271*, 2033.
[12] T. Kamata, K. K. Tieu, A. Irie, T. A. Springer, Y. Takada, *J. Biol. Chem.* **2001**, *276*, 44 275.
[13] Y. Takada, T. Kamata, A. Irie, W. Puzon-McLaughlin, X. P. Zhang, *Matrix Biol.* **1997**, *16*, 143.
[14] M. A. Dechantsreiter, E. Planker, B. Matha, E. Lohof, G. Holzemann, A. Jonczyk, S. L. Goodman, H. Kessler, *J. Med. Chem.* **1999**, *42*, 3033.
[15] G. Müller, M. Gurrath, H. Kessler, *J. Comput. Aided Mol. Des.* **1994**, *8*, 709.
[16] M. Pfaff, K. Tangemann, B. Muller, M. Gurrath, G. Muller, H. Kessler, R. Timpl, J. Engel, *J. Biol. Chem.* **1994**, *269*, 20 233.
[17] J. Emsley, C. G. Knight, R. W. Farndale, M. J. Barnes, R. C. Liddington, *Cell* **2000**, *101*, 47.
[18] W. H. Miller, D. P. Alberts, P. K. Bhatnagar, W. E. Bondinell, J. F. Callahan, R. R. Calvo, R. D. Cousins, K. F. Erhard, D. A. Heerding, R. M. Keenan, C. Kwon, P. J. Manley, K. A. Newlander, S. T. Ross, J. M. Samanen, I. N. Uzinskas, J. W. Venslavsky, C. C. Yuan, R. C. Haltiwanger, M. Gowen, S. M. Hwang, I. E. James, M. W. Lark, D. J. Rieman, G. B. Stroup, *J. Med. Chem.* **2000**, *43*, 22.
[19] S. Honda, Y. Tomiyama, N. Pampori, H. Kashiwagi, T. Kiyoi, S. Kosugi, S. Tadokoro, Y. Kurata, S. J. Shattil, Y. Matsuzawa, *Blood* **2001**, *97*, 175.
[20] A. P. Mould, J. A. Askari, M. J. Humphries, *J. Biol. Chem.* **2000**, *275*, 20 324.
[21] J. D. Humphries, J. A. Askari, X. P. Zhang, Y. Takada, M. J. Humphries, A. P. Mould, *J. Biol. Chem.* **2000**, *275*, 20 337.
[22] D. D. Hu, C. F. Barbas, J. W. Smith, *J. Biol. Chem.* **1996**, *271*, 21 745.
[23] D. D. Hu, J. R. Hoyer, J. W. Smith, *J. Biol. Chem.* **1995**, *270*, 9917.
[24] M. A. Dechantsreiter, E. Planker, B. Mathä, E. Lohof, G. Hölzemann, A. Jonczyk, H. Kessler, *J. Med. Chem.* **1999**, *42*, 3033.
[25] R. R. Hantgan, C. Paumi, M. Rocco, J. W. Weisel, *Biochemistry* **1999**, *38*, 14 461.
[26] J. P. Gallivan, D. A. Dougherty, *Proc. Natl. Acad. Sci. USA* **1999**, *96*, 9459.
[27] A. Sali, T. L. Blundell, *J. Mol. Biol.* **1993**, *234*, 779.
[28] P. Koehl, M. Delarue, *J. Mol. Biol.* **1994**, *239*, 249.
[29] G. M. Morris, D. S. Goodsell, R. S. Halliday, R. Huey, W. E. Hart, R. K. Belew, A. J. Olson, *J. Comput. Chem.* **1998**, *19*, 1639.

Received: January 15, 2002 [Z 344]